v. 4, n. 11, 2024

Journal of
Engineering
Research

EXPERIMENTAL AND NUMERICAL STUDY OF ELETRODEPOSITION PHENOMENA OF COBALT-TUNGSTEN (CO-W) METAL ALLOYS

Nathalia Cristina Ramos Lima
Faculdade de Engenharia Química,
Universidade Estadual de Campinas
São Paulo, Brasil

Ambrósio Florêncio de Almeida Neto
Faculdade de Engenharia Química,
Universidade Estadual de Campinas
São Paulo, Brasil

All content in this magazine is licensed under a Creative Commons Attribution License. Attribution-Non-Commercial-Non-Derivatives 4.0 International (CC BY-NC-ND 4.0).

Abstract: Among the constant problems in petroleum and natural gas engineering, severe corrosion issues are observed in equipment used for storage, transportation, and production of oil and its derivatives. These problems are generated by various mechanisms such as stress from mechanical loads or compounds found in their composition. These occurrences can lead to accidents involving human lives, environmental disasters, and economic losses. As a means of mitigating this problem, the electrodeposition of metallic coatings has proven to be an economical option for covering metal structures, especially when it comes to tungsten-based coatings combined with iron group ions (Ni, Fe, Co).The literature reports few studies on electrodeposition from the perspective of numerical analysis and computer simulation, which would provide a better understanding of the effectiveness and properties of these materials. Therefore, this work aimed to study the numerical and experimental analysis of the steady-state behavior of electrodeposition while conducting experiments on the deposition of the Co-W alloy. The goal was to evaluate the phenomenon of diffusion and forced convection. In this context, results of deposition rates were obtained with magnitudes similar to experimental rates, proving that the analysis is compatible with reality. Another interesting point was the use of both techniques and how the influences of concentration and rotation acted together, showing synergy between the results. In the experimental part, the best coating, with the highest efficiency, was obtained at 30 rpm, 0.15 mol/L sodium tungstate, and pH 6. The simulation identified, just like the experimental results, that a concentration of 0.15 mol/L is ideal, emphasizing that concentration is the most influential factor in the process.
Keywords: Electrodeposition, Tungsten alloy, Forced convection, Numerical analysis.

INTRODUCTION

According to the latest data, equipment in the industry, especially in the petrochemical sector, experiences various forms of corrosion. Among the causes of this phenomenon is the action of chloride ions from seawater. Motivated by the economic importance of this industry and the damages caused by the mentioned factors, many technologies have been developed with the aim of reducing or inhibiting corrosion in these highly aggressive environments [1].

Electrodeposition has been emerging as an effective and viable alternative due to the low amount of electrodeposited material, resulting in a thin and relatively pore-free coating. The most used metals for coating metallic surfaces are Cu, Ni, and Cr [2]. However, tungsten (W) and its metal alloys exhibit very interesting characteristics, such as high corrosion resistance, hardness even at high temperatures, high density, the lowest coefficient of thermal expansion among all metals, and high thermal conductivity [3].

Nevertheless, it is not possible to electrodeposit pure tungsten, either through aqueous electrochemical baths or oily electrolytic baths [4,5]. This occurs due to the codeposition of hydrogen and the fact that tungsten is a reluctant metal to electrodeposit [6]. However, this phenomenon can occur with metals from the iron group (e.g., Fe, Co, Ni, and others), and it is performed without major difficulties through the "induced codeposition" process [7]. In this process, tungsten is added to the electrolyte in the form of tungstate, and then it is added to the metallic salts of the iron group, along with a complexing agent [8].

Although the literature does not report studies that address the electrodeposition of tungsten alloys from a computational perspective using the equations used in this work, it is possible to find studies such

as that of Barbosa [9],who simulated the electro-deposition parameters using the Butler-Volmer equation, or even Frank [10], who used the Kinetic Monte Carlo method to understand the initial stages of cobalt electrodeposition on carbon and copper electrodeposition on gold.

Considering the above, this project proposes the study and development of mathematical models in the computational area for the electro-deposition system of Co-W alloy, in which convective mass transport phenomena are relevant due to cathodic rotation or movement of the electrolytic bath. Using software, a mass transfer model will be constructed that can describe, simulating, and reproducing experimental results. The results will not only allow for the evaluation of the electro-deposition process simulations but also assist in determining the molar deposition fluxes obtained experimentally to validate the evaluated mathematical model. The research will encompass the application of mass transfer fundamentals and the chrono-potentiometric electrodeposition technique.

ELECTRODEPOSITION PHENOMENON

Despite being a natural phenomenon in various materials, including metals and metal alloys, when exposed to aggressive environments, corrosion is a recurring problem in various industrial sectors such as petrochemical, naval, construction, and transportation. The occurrence of corrosion can lead to significant economic losses and even safety risks, as in the case of metallic structures that may lose their load-bearing capacity. According to Groysman [11],corrosion is one of the main challenges faced by the modern industry.

As pointed out by Fontana and Greene [12],understanding the different types of corrosion is fundamental for the identification and prevention of failures in materials and metallic structures. Corrosion is the inverse process to the acquisition of a metal, meaning that the energy that is absorbed spontaneously will be given back or released into the environment, as demonstrated by Eq. 1.

$$Metal + Ambient\ conditions \underset{Corrosion}{\longleftrightarrow} M_e^{Z+} + Energy \quad (1)$$

Electrochemical corrosion is a process that can cause significant damage in various industrial sectors, including the petrochemical, naval, and aerospace industries. In equipment and metallic structures exposed to corrosive environments, corrosion can lead to a reduction in the thickness of the metal, compromising mechanical strength and equipment lifespan. This form of corrosion occurs due to electrochemical reactions involving the metal, the electrolyte, the oxygen present in the environment, and an electrical circuit. Among the various types of corrosion, electrochemical corrosion is one of the most common and can be influenced by various factors, such as temperature, humidity, and acidity of the environment [13].

All electrochemical reactions result from electric currents that depend on the potential difference between two phases (metal and aqueous phase). These reactions occur at the interface, known as the electrical double layer [14].

After a simplified understanding of the reactions, it becomes clear the role and importance that the aqueous solution plays in the process of electrochemical corrosion since it acts as a conductor of positive and negative ions between the metal and the external environment.

STUDY OF ELECTRODEPOSITION IN COBALT-TUNGSTEN (CO-W) ALLOYS

EXPERIMENTAL CAMPAIGN

SUBSTRATE PREPARATION

In order to understand the behavior of the electrodeposition phenomenon in *Co-W* alloys, the substrates were initially prepared. Carbon steel substrates were prepared as cutouts from a SAE 1020 carbon steel sheet as shown in Fig. 1.

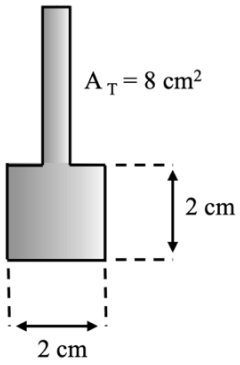

Fig. 01: Steel substrate used to conduct the experiments.

After defining the substrate to be used for the experiments, it was mechanically treated to standardize its surfaces. In addition to mechanical treatment, sodium hydroxide was used (*NaOH* – 10 %) and sulfuric acid (H_2SO_4 – 1 %) to eliminate fats and activate the surface, respectively, aiming for greater adhesion to the study substrate layer. This treated substrate assumed the role of cathode in an electrolytic cell for the development of experiments.

PREPARATION OF ELECTROSTATIC BATHS

Having defined the study body (Fig. 1), the next step is to prepare the electrolytic baths for deposition of coating material on the carbon steel substrate. As a starting point, a metallic specification stage was carried out to verify the balance of chemical components depending on pH. Electrolytic baths were obtained from dissolving sodium tungsten (Na_2WO_4) with concentrations between 0.05 and 0.25 mol/L, this being the source of tungsten. Along with this, sodium borate was added ($Na_2B_4O_7$) at 3.75×10^{-2} mol/L as a source of boron to obtain an amorphous alloy, sodium 1-dodesulfate ($NaC_{12}H_{25}SO_4$) at 1.04×10^{-4} mol/L as a surfactant so that the H_2 released during electrodeposition quickly releases so that it does not form bubbles. In addition to these, ammonium sulfate was added ($(NH_4)_2SO_4$) a 1.287×10^{-1} mol/L to add greater stability to the solution, ammonium citrate ($(NH_4)_2C_6H_6O_7$) at 0.3 mol/L as a complexing agent and cobalt sulfate ($CoSO_4$) as a source of cobalt for electrodeposition at 0.3 mol/L in all verified solutions.

Knowing the solutions used, metal specification diagrams were created using the Hydra software to check the chemical balance as a function of pH. This study is relevant to understand the effect of pH and thus determine the most relevant conditions for experimental verification during the electrodeposition study. Fig. 2 shows the diagram relating to the chemical species of cobalt in the electrolytic bath as a function of pH.

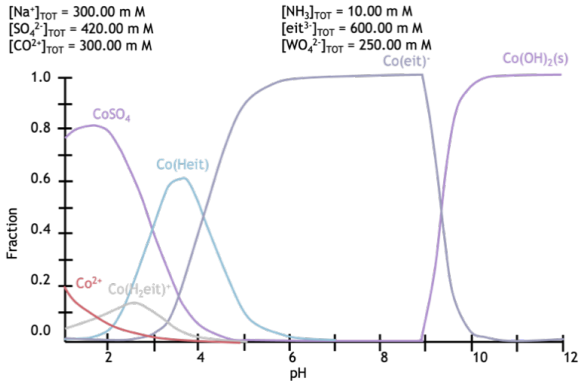

Fig. 2: Cobalt species as a function of pH for a concentration of 0.3 mol/L.

The results in Fig. 2 indicate that they are complexed by ammonium citrate (*Co(cit)*$^{-}$) for pH values between 5 and 8.5, which indicates that the formation of the Co-W alloy can be facilitated under these conditions.

Fig. 3 presents the results of tungsten metal specification for three different concentrations. The W species transitioned to tungsten at pH values between 5.5 and 6, a result similar to that presented by Santana et al. [15].

The results reported in Figs 2 – 3 indicate that pH conditions should be maintained close to 6, this result agrees with information reported by Tsyntasu et al. [16]. Thus, during experimental planning, pH equal to 6 was indicated as the central point (2^3 factorial).

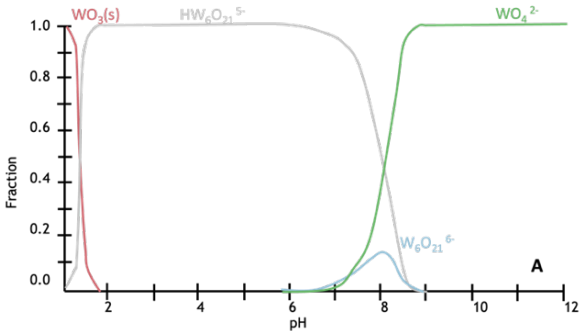

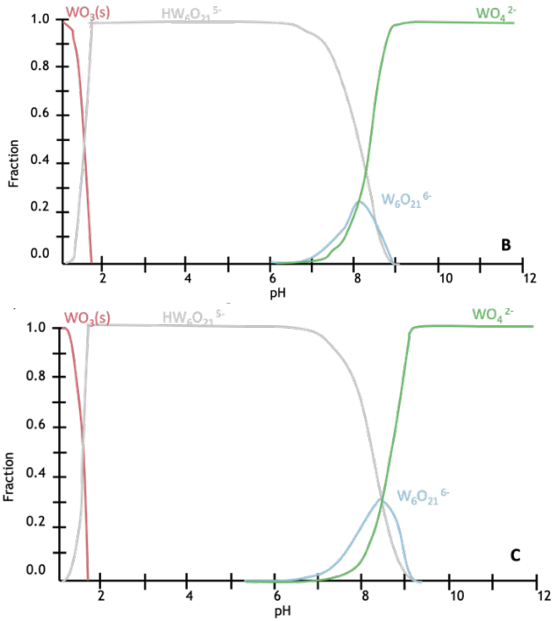

Fig. 3: Especificação metálica de tungstênio (A: 0.05 mol/L; B: 0.15 mol/L; C: 0.25 mol/L).

ELECTRODEPOSITION TESTS

Having knowledge of the electrostatic solutions and the substrate to be used, the next step is to perform the electrodeposition experiment. The system consists of a rotating electrode, a potentiometer for identifying and controlling the difference in electrical potential between the electrode and the counter electrode, as well as a pH measurement. The potentiostat was used as a galvanostat and the counter electrode was a hollow platinum mesh.

The electrodeposition tests were conducted by setting the electrical current density at 10 mA/cm^2 and the average temperature at 25 °C, following recommendations reported by Baldessin et al. [17]. The experimental design proposed to verify the effects of tungstate concentration, cathodic rotation, and pH on the electrodeposition phenomenon. Eight experiments were defined in which the central point was repeated in triplicate, thus totaling 11 experiments.

Electroplating Efficiency

As a metric for evaluating the electrodeposition experiment, the electrodeposition efficiency (ε) was verified as described in Eq. 2.

$$\varepsilon = \frac{m.F}{i.t}\sum\frac{n_j w_j}{M_j} \qquad (2)$$

Where m is the mass of the deposit in grams (g), t is the deposition time in seconds (s), i is the total current used in Amperes (A), w_j is the mass fraction of metal j in the alloy given by EDX (X-Ray Dispersative Energy), n_j is the number of electrons transferred from each atom of metal j, M_j is the atomic mass of metal j in g/mol and F is Faraday's constant (96.485 Coulomb/mol).

The coated substrates were characterized with the aim of understanding the alloy compositions, homogeneity, crystallinity, topography of the deposits and to identify possible contamination from non-metallic substances. After the electrodeposition tests, the coated material will be ready and it is now possible to check the efficiency of the coated metal against corrosion.

NUMERICAL TREATMENT OF THE ELECTRODEPOSITION PHENOMENON

In order to verify the behavior of the electrodeposition phenomenon for conditions that go beyond the experimentally verified conditions, the process in question was modeled considering the control volume presented in Fig. 4.

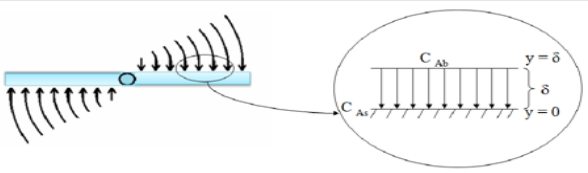

Fig. 4: Forced convection with diffusion to the surface.

The flow of ionic chemical species resulting from forced convection through the rotation (ω) of one of the electrodes around the axis can be described as seen in Fig. 4, where diffusion follows the direction of fluid flow. In electrodeposition systems, the forced convection generated by the rotation of an electrode causes the diffusion of ionic chemical species, such as "A", to occur from the fluid to the surface of the electrode in a steady state. The analysis of the variation in the concentration of "A" requires the evaluation of the molar flow rate in relation to the surface of the material. The concentration varies with the y direction, and close to the surface, the curvature of the concentration profile is neglected, allowing the representation of diffusion in rectangular coordinates.

The molar flow rate of component A towards the *y* axis can be written as a function of the molar flow (W_{Ay}) in the direction normal to the flow (A_c) as described in Eq. 3.

$$F_{Ay} = A_c W_{Ay} \qquad (3)$$

The molar flow of A in the y direction (W_{Ay}) can be written as a function of the diffusivity of A in an incompressible medium B (D_{AB}) as described in Eq. 4.

$$W_{Ay} = -D_{AB}\frac{dC_A}{dy} + u_y C_A \qquad (4)$$

Having knowledge of Eqs. 3 – 4, it is possible to write the molar flow rate of A in the y direction (F_{Ay}) as a function of the diffusivity of A in an incompressible medium B (D_{AB}) and the vector component of velocity in the y direction (u_y).

To describe the variation in the concentration of component A in the y direction, the continuity equation (Eq. 5) will be applied.

$$\frac{\partial C_A}{\partial t} + u_x \frac{\partial C_A}{\partial x} + u_y \frac{\partial C_A}{\partial y} + u_z \frac{\partial C_A}{\partial z} = D_{AB}\left[\frac{\partial^2 C_A}{\partial x^2} + \frac{\partial^2 C_A}{\partial y^2} + \frac{\partial^2 C_A}{\partial z^2}\right] + R_A \quad (5)$$

In addition to considering the consideration of one-dimensional effects, for the purpose of simplifying numerical treatment, the stationary state can be adopted as a hypothesis in addition to the non-existence of possible chemical reactions, thus, the continuity equation (Eq. 5) can be rewritten as presents Eq. 6.

$$u_y \frac{\partial C_A}{\partial y} = D_{AB}\left[\frac{\partial^2 C_A}{\partial y^2}\right] \quad (6)$$

It is now possible to verify the behavior of the concentration of component A with the y direction. To solve Eq. 6, it is necessary to consider the boundary conditions described in Fig. 7 and these are presented in Eqs. 7 – 8.

$$y = 0 \rightarrow C_A = C_{AS} \quad (7)$$

$$y = \delta \rightarrow C_A = C_{AB} \quad (8)$$

The optimization routine for obtaining concentration profiles was implemented in *Python* with the help of the *Scipy* library. The values of the diffusivity coefficients of ions at infinite dilution were obtained from Yuan-Hui and Gregory [18].

Having knowledge of the experimental procedure for preparing the substrate, deposition procedure, preparation of the Co-W alloy and the numerical model for predicting the electrodeposition phenomenon, the following section presents the results obtained following the methodologies described.

RESULTS

RESULTS OF THE EXPERIMENTAL STUDY OF THE ELECTRODEPOSITION PHENOMENON

As the first result to be verified, the Fe-W deposition study will be verified. Table 2 presents the experimental results obtained following the proposed experimental design.

Given the results presented in Table 1, it is possible to verify the combined effects of CT (mol/L), pH and ω (rpm) on the variables of interest. Fig. 5 presents response surfaces to verify the combined effects of manipulable variables on m_{Fe} (g), mW (g) and ε (%).

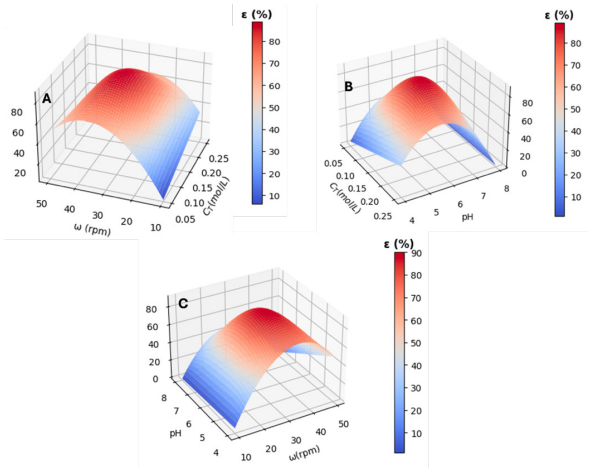

Fig. 5: Response surfaces for combined effects of C_T (mol/L), pH and ω (rpm) on efficiency (A: ε as a function of C_T and w; B: ε as a function of C_T and pH; C: ε as a function of w and pH).

The results in Fig. 5 indicate that all verified variables have effects on the electrodeposition efficiency with visible global maximum points, as a main conclusion, the efficiency is maximized for intermediate conditions of both verified variables. The other variable profiles (m_{Fe} and m_w) are not presented in this text as they present behavior similar to efficiency depending on the variables verified.

Exp.	C_T (mol/L)	ω(rpm)	pH	m_{Fe} (g)	m_W (g)	ε (%)
1	0.05 (-1)	10 (-1)	4 (-1)	0.0030	0.0005	3.91
2	0.25 (+1)	10 (-1)	4 (-1)	0.0249	0.0045	33.33
3	0.05 (-1)	50 (+1)	4 (-1)	0.0360	0.0072	48.92
4	0.25 (+1)	50 (+1)	4 (-1)	0.0181	0.0034	24.44
5	0.05 (-1)	10 (-1)	8 (+1)	No deposition	--	--
6	0.25 (+1)	10 (-1)	8 (+1)	No deposition	--	--
7	0.05 (-1)	50 (+1)	8 (+1)	No deposition	--	--
8	0.25 (+1)	50 (+1)	8 (+1)	No deposition	--	--
9	0.15 (0)	30 (0)	6 (0)	0.0663	0.0120	88.55
10	0.15 (0)	30 (0)	6 (0)	0.0646	0.0121	86.70
11	0.15 (0)	30 (0)	6 (0)	0.0682	0.0121	90.88

Tabela 1: Experimental results for deposition test following the experimental design.

The maximum efficiency point (90.88%) is obtained at pH equal to 6, ω equal to 30 rpm and CT equal to 0.15 mol/L. This result follows the notes of Santana et al.[15] where the author indicated that a pH equal to 6 allows greater results for electrodeposition efficiency. It is verified that for pH values close to 8 there is no electrodeposition, a result that is consistent with verifications carried out by Tsyntsaru et al. [16].

HOMOGENEITY STUDY OF CO-W ALLOYS

After preparing the Co-W alloys, they were subjected to energy dispersive X-ray (EDX) characterization tests to understand the compositions of the alloys in different regions of the plates. Table 2 presents results of the compositions for faces 1 and 2.

The results obtained by EDX for the compositions of the plates indicate that for face 1 the compositions are homogeneous throughout the entire length of the plate, considering that the deviations between the compositions of the center and edge are negligible (Co: 0.88%; W: 5.91 %). This analysis is analogous for side 2 (Co: 1.16 %; W: 5.14 %).

	Center		Between center and edge		Edge	
	Co (at %)	W (at %)	Co (at %)	W (at %)	Co (at %)	W (at %)
Exp.			Face 01			
1	84.04	15.96	83.26	16.74	84.61	15.39
2	85.03	15.97	85.22	14.78	86.03	13.97
3	85.69	14.31	82.72	17.28	86.65	13.35
4	81.77	18.23	83.02	16.98	82.86	17.14
11	85.1	14.9	84.91	15.09	84.99	15.01
			Face 02			
1	85.97	15.03	84.96	15.04	85.12	14.88
2	83.49	16.51	84.58	15.42	85.83	14.17
3	85.43	14.57	83.27	16.73	85.69	14.31
4	82.78	17.22	83.99	16.01	82.02	17.98
11	83.98	16.02	84.26	15.74	84.68	15.32

Tabela 2: Co-W alloy compositions by EDX for faces 1 and 2.

CRYSTALLINITY STUDY OF METALLIC ALLOYS

Crystallinity analyzes were obtained through X-ray diffraction (XRD) tests. Fig. 6 presents results of X-ray diffraction spectra for metallic alloys (Fig. 6A) and for the Co-W alloy from experiment 11 as this was the experiment with the highest efficiency.

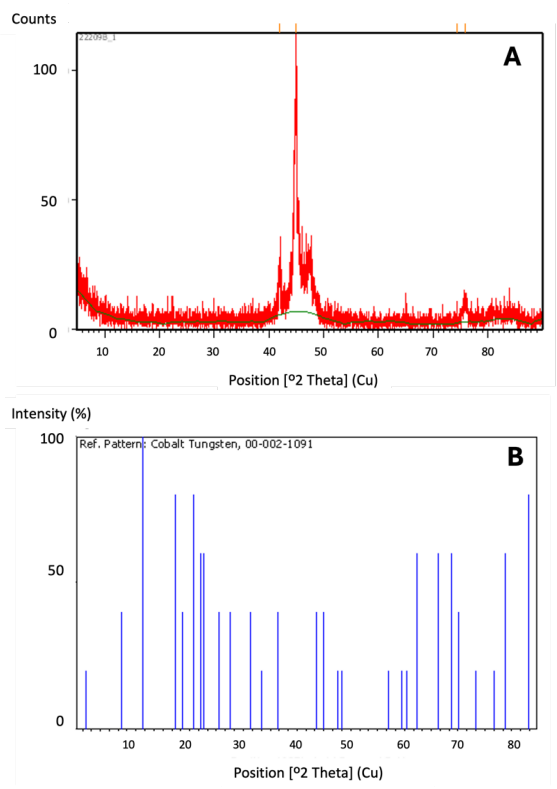

Fig. 6: X-ray diffraction spectra (A: metallic alloys; B: reference Co-W).

From the results in Fig. 6A, it is possible to observe the formation of an upper peak at around 45°, a result that confirms the existence of a crystalline structure and another peak at 42° that concerns the carbon steel substrate, emphasizing its coating.

Comparing the results in Fig. 6B with the results obtained for the Co-W alloy, it is possible to observe the existence of a peak at 42° which indicates that there was indeed coating of the substrate, however, there is no indication of crystallinity.

Based on the results indicated in this section and the information presented in previous literature, it is expected that the alloys tested in this study will present amorphous characteristics, demonstrating high thermal and electrical conductivity, high toughness, and excellent corrosion resistance properties [19,20].

STUDY OF ALLOY MORPHOLOGY

Fig. 7 presents results from scanning electron microscopy (MEV) tests at 1,500 times magnification for experiments 1 (Fig. 7A) and 11 (Fig. 7B). Experiment 1 (Fig. 7A) presented a deposited tungsten mass of 5×10^{-4} g and an efficiency of 3.91%, making it the experiment with the lowest efficiency. Conversely, experiment 11 (Fig. 7B) showed better efficiency (90.88%) with tungsten deposition equal to 1.21×10^{-2} g, for this reason Fig. 9 presents the results for comparing the micrographs.

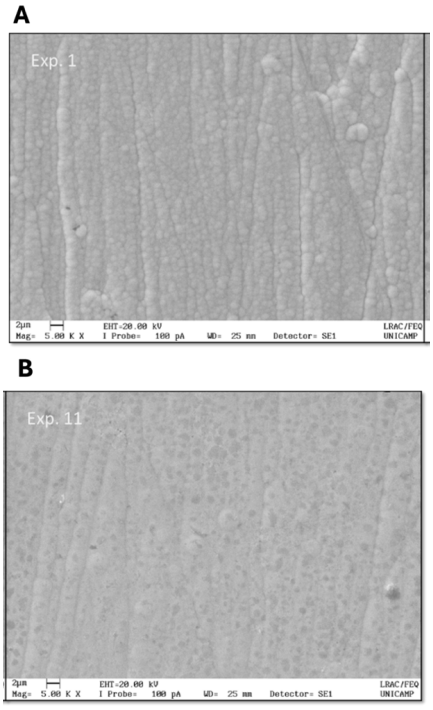

Fig. 9: Micrographs of Co-W alloys (A: experiment 1; B: experiment 11).

The results in Fig. 7 indicate that the coating granules for experiment 1 are larger than those observed for experiment 11, indicating that the increase in W content generated a decrease in size, as was also observed by [16].

Other tests (2, 3 and 4) showed obvious cracks as can be seen in Fig. 8. These results highlight weaknesses in the alloy and these defects can compromise the performance of

the corrosion protection film, allowing the corrosive medium to communicate with the substrate. The existence of the cracks can be justified by the difference in the atomic radius of W due to Co.

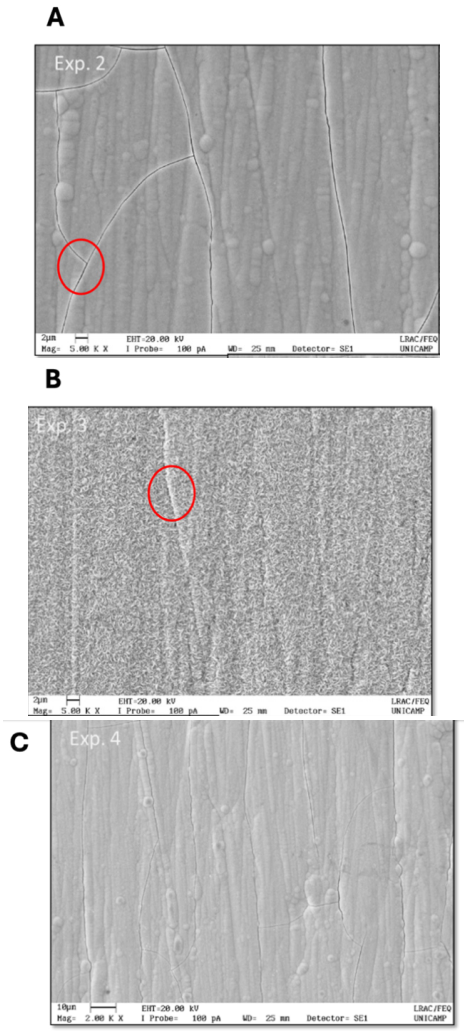

Fig. 8: Micrographs of the Co-W alloys (A: experiment 2; B: experiment 3; C: experiment 4).

3.2. Results of the numerical study of the electrodeposition phenomenon

The numerical problem consists of solving the differential equation presented in Eq. 6. This section presents the results obtained for the concentration (CA) and molar flow (W) profiles as a function of length in y (Fig.4).

One factor to be considered is that the proposed equation does not take into account the effects of the pH of the medium, for this reason considerable deviations are expected in relation to the experimental results given that pH has a major effect on the concentration behavior.

The result in Fig. 9A refers to the simulated result following the conditions of experiment 11, which was conducted at 10 rpm at a sodium tungsten concentration equal to 0.05 mol/L. Fig. 9B presents the simulated results under experimental conditions for the central point at 30 rpm with sodium tungsten concentration equal to 0.15 mol/L. Inicialmente observa-se que um comportamento linear da concentração e do fluxo molar em função de *y*, o que é esperado devido a transformação dos compostos em filmes eletrodepositados.

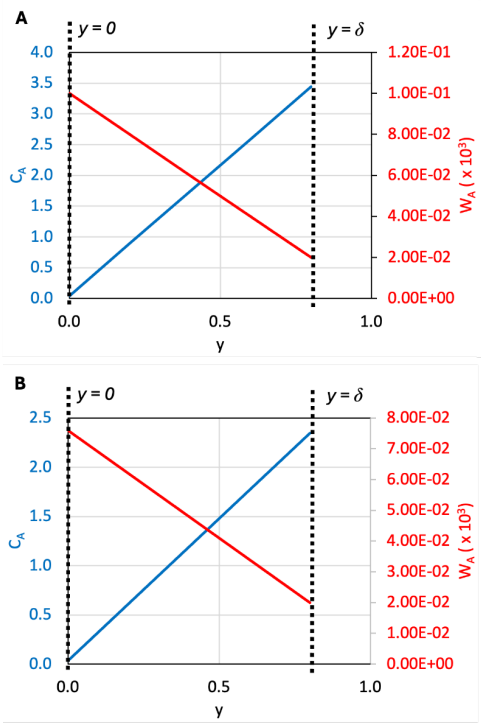

Fig. 9: Behavior of molar flow concentration as a function of y for experiment 1 (A) and for the central point (B).

Applying the same simulation methodology to verify the concentrations and molar flux of cobalt, the results are similar where the molar flux is always decreasing, and the concentration is always increasing. Table

				Experimental		Simulated	
Exp.	C_T (mol/L)	ω(rpm)	pH	W	Co	W	Co
1	0.05 (-1)	10 (-1)	4 (-1)	2.53E-03	4.82E-03	2.67E-05	2.03E-05
2	0.25 (+1)	10 (-1)	4 (-1)	1.27E-04	4.79E-03	5.34E-02	2.03E-05
3	0.05 (-1)	50 (+1)	4 (-1)	1.26E-04	2.39E-04	2.34E-05	1.61E-05
4	0.25 (+1)	50 (+1)	4 (-1)	6.33E-04	2.40E-04	4.59E-05	1.61E-05
5	0.05 (-1)	10 (-1)	8 (+1)	No deposition		-	-
6	0.25 (+1)	10 (-1)	8 (+1)	No deposition		-	-
7	0.05 (-1)	50 (+1)	8 (+1)	No deposition		-	-
8	0.25 (+1)	50 (+1)	8 (+1)	No deposition		-	-
9	0.15 (0)	30 (0)	6 (0)	2.28E-04	1.42E-04	1.50E-05	1.47E-05
10	0.15 (0)	30 (0)	6 (0)	2.28E-04	1.43E-04	1.50E-05	1.47E-05
11	0.15 (0)	30 (0)	6 (0)	2.28E-04	1.42E-04	1.50E-05	1.47E-05

Table 8. Comparison between simulated and experimental results for concentration and molar flow.

3 presents the comparison between the experimental and simulated results obtained for concentrations and molar flow. As expected, the deviations between these are significant and this is justified by the fact that the numerical methodology adopted does not consider all possible effects on the phenomenon under study. However, the order of magnitude behavior remained consistent with changes in rotation.

CONCLUSIONS

At the conference on numerical and experimental analysis, notable discrepancies are evident, residing in system variables inadequately considered in the equations used. A notable example is pH, a factor that can play a crucial role in system dynamics but may be overlooked in numerical modeling. The pH can influence the solubility of chemical species, chemical reactions, and even electron availability in the system, thus affecting molar flow outcomes.

The focal point of experimental design yielded the best deposition efficiency results (90.88%), and for molar flow, it proved to be intermediary, aligning with 2^3 design experimental design. In the numerical analysis conducted, comparing different scenarios involving variable changes, it's evident that concentration exerts a more significant influence than rotation on tungsten compound behavior. This suggests that, for this compound, concentration variation is the determining factor in its properties and behavior. However, examining the cobalt compound, we note that the only variable altered was rotation. In this case, this experimental approach allowed us to isolate the impact of rotation on cobalt compound properties and behavior. Results from this simulation clearly indicate that, in the context of this research, compound concentration exerts a more significant influence than rotation. These findings are highly relevant as they underscore the importance of considering concentration as a predominant factor in tungsten compound analysis, whereas for cobalt compound, rotation variation is the central aspect to be considered. This knowledge significantly contributes to a more precise and comprehensive understanding of these compounds' behavior in various contexts and applications.

CONFLICT OF INTEREST

On behalf of all authors, the corresponding author states that there is no conflict of interest.

REFERENCES

[1] Luiz LA, Henke SL, Kurelo BCES, Souza GB de, Andrade J de, Marino CEB. AÇOS INOXIDÁVEIS APLICADOS NA INDÚSTRIA PETROQUÍMICA: ESTUDO COMPARATIVO DA RESISTÊNCIA À CORROSÃO POR TÉCNICAS ELETROQUÍMICAS. Tecnol Metal Mater Min 2020;17:61–70. https://doi.org/10.4322/2176-1523.20201960.

[2] Abdel Hamid Z. Electrodeposition of cobalt–tungsten alloys from acidic bath containing cationic surfactants. Mater Lett 2003;57:2558–64. https://doi.org/10.1016/S0167-577X(02)01311-3.

[3] Bhattarai J, Akiyama E, Habazaki H, Kawashima A, Asami K, Hashimoto K. Electrochemical and XPS studies on the passivation behavior of sputter-deposited W-Cr Alloys in 12 M HCl solution. Corros Sci 1998;40:155–75. https://doi.org/10.1016/S0010-938X(97)00106-6.

[4] Paunovic M, Schlesinger M. Fundamentals of electrochemical deposition. john wiley & sons; 2006.

[5] Davis GL, Gentry CHR. The electrodeposition of tungsten. Metallurgia 1956;53:3.

[6] MOREIRA FL, PORTO MB, VIEIRA MGA, SILVA MGC DA, NETO AFDA. OBTENÇÃO E CARACTERIZAÇÃO DE LIGAS DE FE-W DESTINADAS À PROTEÇÃO ANTICORROSIVA. Anais do XXXVII Congresso Brasileiro de Sistemas Particulados, São Paulo: Editora Edgard Blücher; 2015, p. 192–7. https://doi.org/10.5151/ENEMP2015-FI-412.

[7] Brenner A. Electrodeposition of alloys: principles and practice. Elsevier; 2013.

[8] Argañaraz MPQ, Ribotta SB, Folquer ME, Gassa LM, Benítez G, Vela ME, et al. Ni–W coatings electrodeposited on carbon steel: Chemical composition, mechanical properties and corrosion resistance. Electrochim Acta 2011;56:5898–903. https://doi.org/10.1016/j.electacta.2011.04.119.

[9] BARBOSA WA. Estudo experimental e simulado de eletrodeposição da Liga Ni-W. 2008.

[10] Frank A, Heidemann W, Spindler K. Modeling of the surface-to-surface radiation exchange using a Monte Carlo method. J Phys Conf Ser 2016;745:032143. https://doi.org/10.1088/1742-6596/745/3/032143.

[11] Groysman A. Corrosion in systems for storage and transportation of petroleum products and biofuels: identification, monitoring and solutions. Springer Science & Business Media; 2014.

[12] Fontana MG, Greene ND. Corrosion engineering. McGraw-hill; 2018.

[13] Meira GR. Corrosão de armaduras em estruturas de concreto: fundamentos, diagnóstico e prevenção. Editora IFPB; 2017.

[14] Bard AJ, Faulkner LR, White HS. Electrochemical methods: fundamentals and applications. John Wiley & Sons; 2022.

[15] Santana RAC, Oliveira ALM, Campos ARN, Prasad S. Otimização das condições operacionais para eletrodeposição da liga Co-Mo, utilizando planejamento experimental. Revista Eletrônica de Materiais e Processos 2007;2:1–9.

[16] Tsyntsaru N, Cesiulis H, Budreika A, Ye X, Juskenas R, Celis J-P. The effect of electrodeposition conditions and post-annealing on nanostructure of Co–W coatings. Surf Coat Technol 2012;206:4262–9. https://doi.org/10.1016/j.surfcoat.2012.04.036.

[17] Baldessin CF, de Morais Nepel TC, de Almeida Neto AF. The influence of Ni and Co concentration in the electroplating bath on Ni-Co-W alloys properties. Can J Chem Eng 2018;96:1284–9. https://doi.org/10.1002/cjce.23076.

[18] Yuan-Hui L, Gregory S. Diffusion of ions in sea water and in deep-sea sediments. Geochim Cosmochim Acta 1974;38:703–14. https://doi.org/10.1016/0016-7037(74)90145-8.

[19] Askeland DR, Phulé PP, Wright WJ, Bhattacharya DK. The science and engineering of materials 2003.

[20]PORTO MB, VIEIRA MGA, SILVA MGC, NETO AFA. ESTUDO DO COMPORTAMENTO DA EFICIÊNCIA DE DEPOSIÇÃO DA LIGA Co-W UTILIZANDO PLANEJAMENTO EXPERIMENTAL. XXXVII Congresso Brasileiro de Sistemas Particulados, 2015, p. 184–91.